Macromolecules
ARTICLE

Macromolecules **2010**, *43*, 8511–8518 **8511**
DOI: 10.1021/ma1015352

"Functional Poly(ethylene glycol)": PEG-Based Random Copolymers with 1,2-Diol Side Chains and Terminal Amino Functionality

Christine Mangold,[†] Frederik Wurm,[‡] Boris Obermeier,[†] and Holger Frey*[,†]

[†]*Institute of Organic Chemistry, Organic and Macromolecular Chemistry, Duesbergweg 10-14, Johannes Gutenberg-Universität Mainz, D-55099 Mainz, Germany, and* [‡]*Institut des Matériaux, Laboratoire des Polymères, Batiment MXD, Station 12, Ecole Polytechnique Fédérale de Lausanne, CH-1015 Lausanne, Switzerland*

Received July 9, 2010; Revised Manuscript Received September 15, 2010

ABSTRACT: A series of poly(ethylene glycol-*co*-isopropylidene glyceryl glycidyl ether) (P(EO-*co*-IGG)) random copolymers with different fractions of 1,2-isopropylidene glyceryl glycidyl ether (IGG) units was synthesized. After acidic hydrolysis a new type of "functional PEGs", namely poly(ethylene glycol-*co*-glyceryl glycerol) (P(EO-*co*-GG)) was obtained. Using an initiator that releases a terminal amino moiety after deprotection, functional end groups with orthogonal reactivity to the in-chain groups were obtained. All polymers showed narrow molecular weight distributions (1.07−1.19), and control of the molecular weights was achieved in the range 5000−30 000 g/mol. Random incorporation of both comonomers was verified by monitoring the copolymerization kinetics via real-time ^{1}H NMR spectroscopy during the polymerization and by characterization of the triad sequence distribution, relying on ^{13}C NMR analysis. Using the 1,2-diol component of the side chains allows for attachment and facile acid-catalyzed release of molecules bearing ketone/aldehyde functionalities. This renders the materials potentially useful as support for reagents, drugs or catalysts. This was demonstrated using benzaldehyde as a model compound. DSC was carried out on all samples, showing amorphous structures upon incorporation of IGG fractions exceeding 15%.

Introduction

Poly(ethylene oxide) (PEO) is undoubtedly the most important polymer for biomedical applications today. This is based on two major key features: on the one hand PEO shows excellent solubility in aqueous media, and second PEO is biocompatible, possessing low immunogenicity and antigenicity.[1,2] Therefore, PEO, or poly(ethylene glycol) (PEG), which mostly refers to PEO with a molecular weight below 20 000 g/mol and its anionic or cationic derivatives are used in numerous cosmetic[3] and also pharmaceutical products. Furthermore, molecular hybrids of PEG and peptide or protein drugs play an important role to enhance circulation times. The covalent linkage of monofunctional PEG (mPEG) to a variety of different biomolecules is known as "PEGylation" and represents a well established method today,[4,5] which is already standard practice for different medications.

The introduction of functional groups other than hydroxyl to obtain mono- or difunctional PEG derivatives can either be realized by a suitable initiator system or via appropriate terminating agents in the anionic ring-opening polymerization of ethylene oxide (EO). A detailed overview has been given by Riffle et al.[6] A newly developed initiator, which allows the introduction of a terminal amino moiety by catalytic hydrogenation subsequent to the polymerization was recently introduced by our group.[7]

The preparation of well-defined PEGs with more than two functional groups that are randomly distributed at the polyether backbone requires a comonomer bearing a protecting group, which must be stable under the strongly basic reaction conditions of the oxyanionic polymerization and can be removed quantitatively in postpolymerization reactions. Suitable comonomers are glycidyl ethers, which release one hydroxyl function per monomer unit upon acidic hydrolysis or catalytic hydrogenolysis. At present the most prominent glycidyl ether is ethoxy ethyl glycidyl ether (EEGE), which was first mentioned by Fitton et al.[8] and has been employed by several groups[9−11] to obtain block[12,13] and recently also random copolymers with EO.[14−16] Möller et al. have reported an elegant synthesis of copolymers using various glycidyl ethers for the orthogonal deprotection of the hydroxyl functionality.[17] For the introduction of other functional groups, two different methods are possible: The first option is the derivatization of hydroxyl-functionalized polymers in subsequent polymer modification reactions.[18] In this case the degree of functionalization strongly depends on the yields and selectivity of the respective modification reactions, often leading to inhomogeneous product mixtures. An alternative approach to functional PEG copolymers relies on the copolymerization of protected epoxide comonomers. In this context, we recently reported the use of the protected amino analogue of glycidol to introduce multiple amino groups via random copolymerization.[19]

While polymerization of the above-mentioned "classical" glycidyl ethers results in linear poly(glycerol)s (*lin*PG) after deprotection, the use of 1,2-isopropylidene glyceryl glycidyl ether (IGG),[20] a monomer that was recently developed in our group, permits the introduction of glycerol side chains with two adjacent hydroxyl functions for each IGG unit incorporated after acidic hydrolysis of the acetal protective groups. To date, the IGG monomer has only been employed in the synthesis of block copolymers or served as precursor for the synthesis of linear-hyperbranched PEG-*b*-*hbpoly*(glycerol) (PG) copolymers.[20,21] However, the presence of two vicinal hydroxyl groups also opens a general pathway for attachment to the chain and facile, acid-catalyzed release of any molecule with a ketone or aldehyde functionality via formation of the cyclic acetal or ketal, respectively. This leads to various interesting applications, such as

*To whom correspondence should be addressed. E-mail: hfrey@uni-mainz.de.

Published on Web 09/29/2010

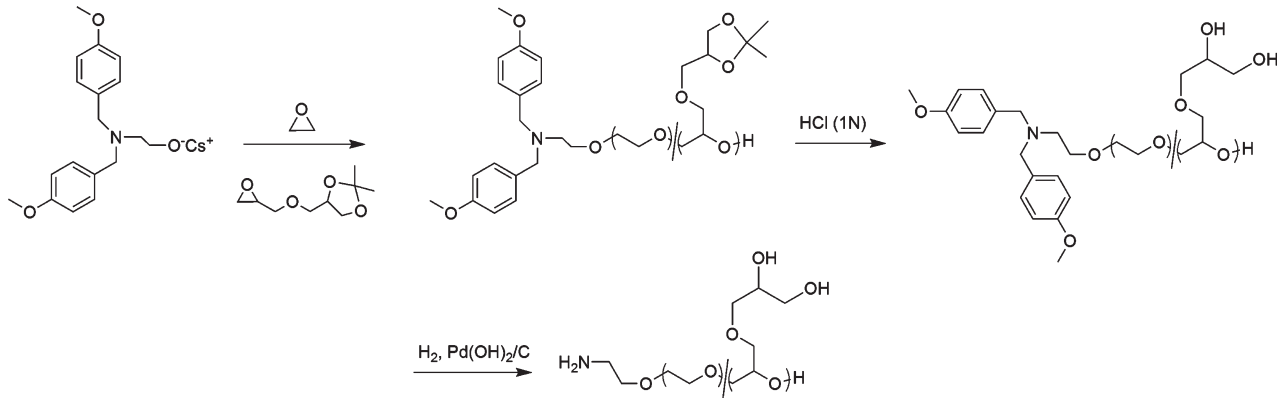

Figure 1. Reaction sequence for the synthesis of the random P(EO-*co*-IGG)-copolymers bearing one single terminal amino- and multiple 1,2-diol side groups.

transport and controlled release of drugs or other biomolecules and furthermore the use of these novel polymers as polymeric support for organic synthesis.

In the current work, we have studied the random copolymerization of the recently introduced, protected comonomer IGG with ethylene oxide by anionic ring-opening copolymerization. Subsequent acidic hydrolysis results in PEG-copolymers with 1,2-diol side chains (Figure 1). Detailed characterization focusing on polymerization kinetics, polymer microstructure and thermal properties is presented. With this work we aim at the following issues: (i) Can both comonomers be copolymerized in a random manner, despite the steric bulk of the IGG comonomer and the high reactivity of EO? (ii) How does copolymerization influence the materials properties of the "functional PEGs" in comparison to PEG? (iii) Can the resulting copolymers be employed for the reversible attachment and acid-catalyzed liberation of a model drug?

Experimental Section

Instrumentation. ^{1}H NMR spectra (300 and 400 MHz) and ^{13}C NMR spectra (75.5 MHz) were recorded using a Bruker AC300 or a Bruker AMX400. All spectra were referenced internally to residual proton signals of the deuterated solvent. For SEC measurements in DMF (containing 0.25 g/L of lithium bromide as an additive) an Agilent 1100 Series was used as an integrated instrument, including a PSS HEMA column ($10^6/10^5/10^4$ g/mol), a UV (275 nm) and a RI detector. Calibration was carried out using poly(ethylene oxide) standards provided by Polymer Standards Service. DSC measurements were performed using a Perkin-Elmer 7 series thermal analysis system and a Perkin-Elmer Thermal Analysis Controller TAC 7/DX in the temperature range from −100 to 80 °C at heating rates of 10 $K \cdot min^{-1}$ under nitrogen. Matrix-assisted laser desorption and ionization time-of-flight (MALDI−ToF) measurements were performed on a Shimadzu Axima CFR MALDI-TOF mass spectrometer using potassium trifluoroacetic acid as a cationizing agent and dithranol (1,8,9-trishydroxyanthracene) as a matrix.

Reagents. All solvents and reagents were purchased from Acros Organics and used as received, unless otherwise stated. Chloroform-d_1 and DMSO-d_6 were purchased from Deutero GmbH. 1,2-Isopropylidene glyceryl glycidyl[20] ether was prepared according to a recently published procedure, dried over CaH_2, and freshly distilled before use.

***p*-Methoxybenzyl Bromide.** A 25 g sample of *p*-methoxybenzyl alcohol (0.21 mol) and 400 mL of dry diethyl ether were placed in 1-L three-neck round-bottom flask and 29 g of phosphorus tribromide (0.11 mol) was added via dropping funnel for 2 h. The reaction mixture was then allowed to stir at room temperature for additional 12 h. Then, 300 g of ice was added to hydrolyze the excess of phosphorus tribromide. The organic and aqueous phases were separated, and the aqueous phase was extracted with 2 × 200 mL of diethyl ether. The combined organic extracts were washed with 300 mL of H_2O and 300 mL of a saturated $NaHCO_3$ solution, dried with $MgSO_4$, and concentrated *in vacuo*. A slightly yellow viscous liquid was obtained, which was then distilled at 13 mbar. Bp: 113 °C. Yield: 35.5 g (83%) ^{1}H NMR (300 MHz, $CDCl_3$), δ (ppm) = 7.33 (d, 2H, aromatic), 6.88 (d, 2H, aromatic), 4.51 (s, 2H, BrCH_2Ph), 3.80 (s, 3H, OCH_3).

***N*,*N*-Di(*p*-methoxybenzyl)aminoethanol.** A 15 g sample of the freshly distilled *p*-methoxybenzyl bromide (75 mmol), 2.3 g of aminoethanol (37 mmol), 13.8 g of K_2CO_3 (100 mmol), and 100 mL of DMF were refluxed for 24 h. After the reaction mixture was allowed to cool to room temperature, the solution was filtrated and 300 mL of diethyl ether was added. The organic phase was then washed with water and a saturated $NaHCO_3$ solution and dried with $MgSO_4$. The organic phase was dried *in vacuo*, and a highly viscous liquid was obtained. The crude mixture was purified by column chromatography using acetic acid ethyl ester and petrol ether as solvents. Yield: 9 g (80% theoretical) ^{1}H NMR (300 MHz, $CDCl_3$): δ (ppm) = 7.33 (d, 4H, aromatic), 6.88 (d, 4H, aromatic), 3.80 (s, 6H, OCH_3), 3.60 (s, 4H, NCH_2Ph), 3.57 (t, 2H,CH_2OH), 2.65 (t, 2H, NCH_2).

General Procedure for the Copolymerization of EO and IGG. *N*,*N*-Di(*p*-methoxybenzyl)-2-aminoethanol was dissolved in benzene in a 250 mL Schlenk flask and 0.9 equiv of cesium hydroxide monohydrate was added. The mixture was stirred at 60 °C under argon for 1 h and evacuated at 90 °C (10^{-2} mbar) for 2 h to remove benzene and water, forming the corresponding cesium alkoxide. Approximately 1 mL dry THF was then cryo-transferred into the Schlenk flask to dissolve the initiator salt. EO was first cryo-transferred to a graduated ampule and then cryo-transferred into the flask containing the initiator in THF (at around −80 °C). Subsequently, the second comonomer (IGG) was added via syringe and the mixture was heated to 60 °C and stirred for 18−24 h. Precipitation in cold diethyl ether resulted in the pure copolymers. For polymers with a high fraction of IGG, the polymer solution was dried *in vacuo*. Yields: 95% to quantitative. ^{1}H NMR (300 MHz, DMSO-d_6): δ (ppm) = 7.24, 6.87 (d, C_6H_4OMe), 4.16 (m, acetal-*H*), 3.98 (t, C*H*H-acetal), 3.74 (s, C_6H_4O*Me*), 3.68−3.34 (polyether backbone), 1.3 (d, CH_3 acetal).

α-*N*,*N*-Di(*p*-methoxybenzyl)−poly(ethylene oxide-*co*-glyceryl glycerol). The acetal protecting groups were removed by the addition of 1 N hydrochloric acid to a 20% solution of the polymer in MeOH/THF 1:1 and about 500 mg of ion-exchange resin (Dowex 50WX8). The reaction mixture was stirred at room temperature for 12 h, filtrated (to remove the resin) and concentrated *in vacuo*. Yields: 80−90%. ^{1}H NMR (300 MHz, DMSO-d_6): δ (ppm) = 7.53, 7.00 (d, C_6H_4OMe), 4.01−3.80 (br, O*H*), 3.74 (s, C_6H_4O*Me*), 3.67−3.09 (polyether backbone).

α-H_2N−poly(ethylene oxide-*co*-glyceryl glycerol) or H_2N−poly(ethylene oxide-*co*-isopropylidene glyceryl glycidyl ether). A 1 g sample of copolymer was dissolved in 50 mL of methanol (or a methanol/THF mixture in the case of the IGG species) and palladium on activated charcoal (10%) was added. The reaction vessel was flushed with hydrogen (8 bar) and the reaction was allowed to stir for 72 h at room temperature. The solution was filtered, concentrated, and precipitated into cold diethyl ether. Yields: quantitative. H_2N−poly(ethylene oxide-*co*-glyceryl glycerol) ^{1}H NMR (300 MHz, DMSO-d_6): δ (ppm) = 4.54 (m, OH, position varies dependent on concentration/temperature etc.) 3.81−3.15 (m, polyether backbone). H_2N−poly(ethylene oxide-*co*-isopropylidene glyceryl glycidyl ether) ^{1}H NMR (300 MHz, DMSO-d_6): δ = 4.16 (m, acetal-*H*), 3.98 (t, C*H*H-acetal), 3.74 (s, C_6H_4OMe), 3.68−3.34 (polyether backbone), 1.3 (d, CH_3 acetal).

***N*,*N*-Di(*p*-methoxybenzyl)−poly(ethylene oxide-*co*-2-phenyl 1,3-dioxolan glycidyl ether).** A 1 g sample of P(EO-*co*-GG) as well as a 10-fold excess (per GG-unit) of benzaldehyde dimethyl acetal was placed in a round-bottom flask. A catalytic amount of *p*-toluenesulfonic acid was added, and the mixture was put into an ultrasonic bath at room temperature and under argon atmosphere for 3 h until a homogeneous mixture was obtained. Piperidine was added, and all volatile compounds were removed under reduced pressure. The crude product mixture was then dialyzed in THF using benzoylated tubing with a molecular weight cut off (MWCO) of 1000 g/mol. After 72 h THF was removed *in vacuo* and the pure copolymer was obtained. Yield: 80%. ^{1}H NMR (300 MHz, DMSO-d_6): δ (ppm) = 7.52−7.33 (m, arom. side-chain), 7.22 (d, C_6H_4OMe), 6.84 (d, C_6H_4OMe), 5.74 (d, acetal-*H*), 4.25−3.25 (m, polyether backbone).

^{1}H NMR Kinetics.[19] In a conventional NMR tube, a mixture of IGG and EO in DMSO-d_6 was placed under an argon atmosphere, cooled to −196 °C, and evacuated. The initiator solution was added rapidly to guarantee that the first layer stayed frozen and no reaction took place. Then the tube was evacuated again while freezing the initiator-solution. The NMR tube was flame-sealed by applying high vacuum. It is of crucial importance to keep both solution-layers frozen until the NMR measurements are started. Immediately after melting and mixing of the two solutions, the first spectrum was recorded. Intervals between two measurements were 5 s within the first minute and extended afterward. A sample of the pure monomer mixture was measured in advance to reduce the necessary time for locking and shimming.

Results and Discussion

Synthesis. To copolymerize two monomers such as EO and IGG with highly diverging boiling points a procedure has to be chosen that levels these differences to a minimum. All reactions were therefore carried out at 60 °C *in vacuo*, as reported recently for another EO copolymerization.[19] There appears to be a general bias that the reactivity of ethylene oxide is generally considerably higher than for all other epoxide monomers, such as glycidyl ethers. It is an important objective of this work to clarify this issue by probing the possibility of random copolymerization in this system that combines EO with a bulky epoxide as a comonomer.

As a novel initiator *N*,*N*-di(*p*-methoxybenzyl)aminoethanol has been prepared. This initiator has been improved in comparison to the previously mentioned *N*,*N*-Dibenzylaminoethanol by introducing methoxy groups in the para-position of the aromatic system, permitting more facile cleavage, which is due to the inductive effect of the methoxy groups. *N*,*N*-Di(*p*-methoxybenzyl)aminoethanol was deprotonated with 0.9 equiv of cesium hydroxide monohydrate, and the polymerization was carried out in a highly concentrated solution of the two monomers and THF. In the NMR online experiments, which were carried out not only to verify the kinetics of the reaction but also the reactivity of the two comonomers, DMSO-d_6 was used as a solvent. This is mainly due to experimental and security reasons with regard to the higher boiling point of DMSO in comparison to THF. Depending on the IGG-content of the samples, the copolymers obtained possessed different appearance, ranging from amorphous solids (9% IGG) to highly viscous liquids (53% IGG), in pronounced contrast to PEG, which is a crystalline powder at room temperature. Detailed characterization of the thermal properties is given in a following section subsequent to the structural characterization of the materials.

Completion of the polymerization was monitored via ^{1}H NMR spectroscopy, relying on the absence of the oxirane-signals corresponding to the two monomers after about 24 h stirring at 60 °C. The copolymer composition was also studied by ^{1}H NMR spectroscopy (Figure 2). Agreement of the IGG fraction incorporated in the random copolymers with the composition of the monomer feed is confirmed by ^{1}H NMR spectra from the comparison of the polyether backbone signals with the acetal protons at 4.16 ppm and the methyl signals centered around 1.3 ppm. In addition, from ^{1}H NMR spectroscopy the number-average molecular weight was calculated by integration of the aromatic resonances of the initiator (6.87 ppm), the polyether backbone (3.5 ppm), and the signals referring to IGG units (1.2 ppm). It should be noted at this point that due to the high molecular weights obtained the error of this method is on the order of 5−10%. Size exclusion chromatography (SEC) was carried out for all copolymer samples, demonstrating narrow molecular weight distributions (M_w/M_n = 1.08−1.19). As can be seen from Table 1, the molecular weights obtained from the SEC measurements using PEG standards deviate from the values calculated from the ^{1}H NMR measurements. The deviation is approximately half of the value for the 10% IGG content samples and becomes gradually more pronounced with increasing amount of IGG incorporated. This is due to the peculiar nature of the molecular weight increase, since the additional groups are located in the side chains, most probably resulting in a stagnating hydrodynamic radius.

Removal of the cyclic protecting group and release of the two adjacent hydroxyl-functionalities in the polymer-backbone was readily achieved under moderately acidic conditions and stirring for 12 h at room temperature. Removal of the protecting groups can be followed by NMR via disappearance of the peaks due to the isopropylidene groups, for instance the acetal proton at 4.16 ppm (^{1}H NMR, Figure 2) or the corresponding carbon atom and its signal at 99 ppm (^{13}C NMR). After release of the hydroxyl functions, the apparent molecular weights obtained from SEC increase for all P(EG-*co*-GG) samples, while a decrease would be expected due to the loss of the acetal group. Interestingly, this increase is directly correlated to the IGG content and therefore to the number of hydroxyl functions formed. This can most likely be attributed to the emerging diol functions that interact with the SEC columns, thus leading to an apparent increase in the hydrodynamic radii (compare with Figure 7). The polydispersities remained low after deprotection and were in the range of M_w/M_n = 1.09−1.19.

Similar to the deprotection of the acetals, the liberation of the terminal amino moiety by catalytic hydrogenation can be followed via ^{1}H NMR, monitoring the disappearance of the aromatic signals at 6.86 and 7.24 ppm. The reaction conditions applied for the hydrogenolysis guarantee removal of the benzylic protecting groups at the amine without removal of the isopropylidene protecting groups. Figure 2 shows the

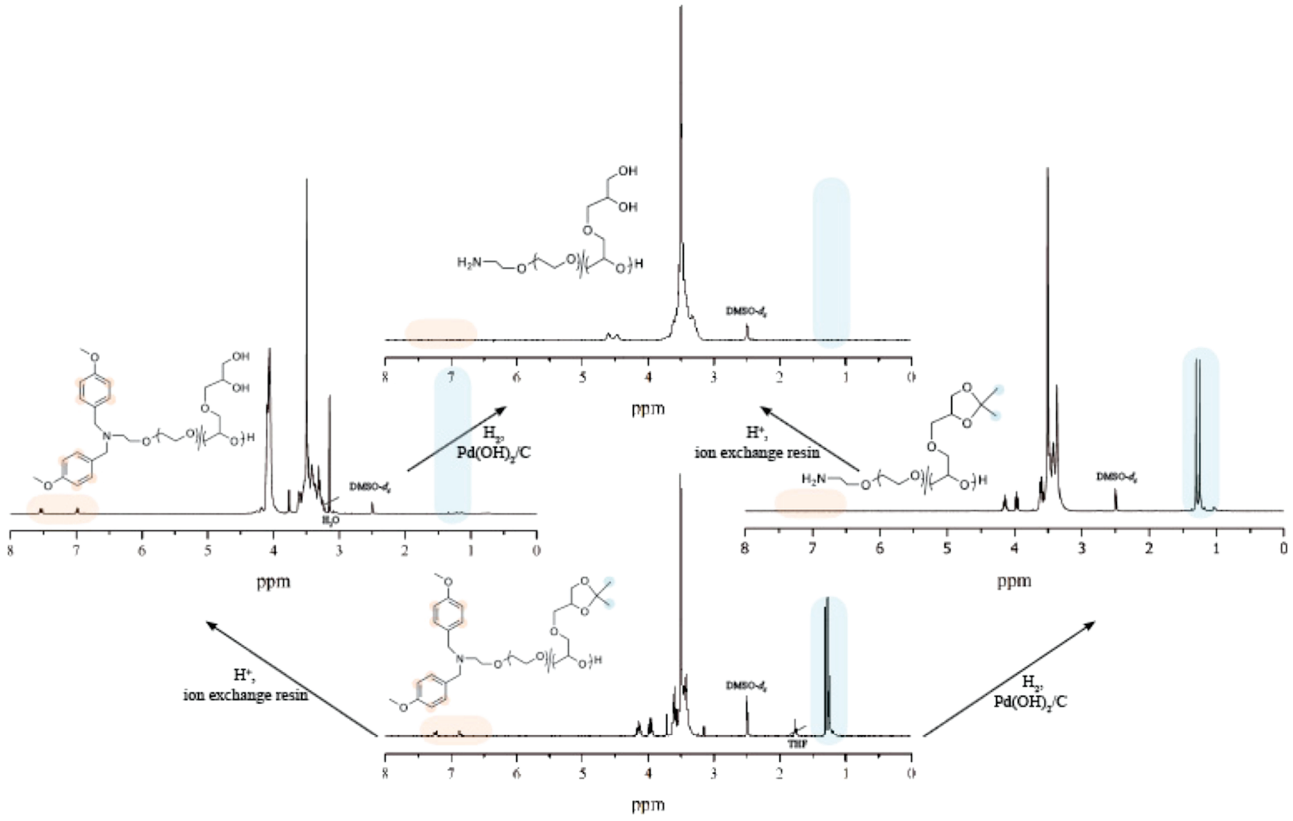

Figure 2. ^{1}H NMR spectra of the copolymers synthesized. The deprotection steps can be interchanged.

Table 1. Overview of the Characterization Data for All Copolymer Samples Prepared

no.	composition (theor)	sum (NMR)[a]	IGG/GG-fraction[a] (%)	M_n (NMR)	M_n (SEC)[b]	PDI (SEC)[b]
1	$MeOBn_2NP(EO_{200}-IGG_{20})$	$MeOBn_2NP(EO_{265}-IGG_{26})$	9	16500	7600	1.11
2	$MeOBn_2NP(EO_{160}-IGG_{40})$	$MeOBn_2NP(EO_{180}-IGG_{32})$	14	14000	7000	1.15
3	$MeOBn_2NP(EO_{45}-IGG_{15})$	$MeOBn_2NP(EO_{47}-IGG_{17})$	26	5300	3000	1.08
4	$MeOBn_2NP(EO_{100}-IGG_{50})$	$MeOBn_2NP(EO_{90}-IGG_{40})$	30	11800	4700	1.11
5	$MeOBn_2NP(EO_{100}-IGG_{100})$	$MeOBn_2NP(EO_{122}-IGG_{136})$	53	30000	4500	1.13
1d	$MeOBn_2NP(EO_{265}-GG_{26})$	$MeOBn_2NP(EO_{265}-GG_{26})$	9	15700	8000	1.15
2d	$MeOBn_2NP(EO_{180}-GG_{32})$	$MeOBn_2NP(EO_{180}-GG_{32})$	14	12800	8700	1.17
3d	$MeOBn_2NP(EO_{47}-GG_{17})$	$MeOBn_2NP(EO_{47}-GG_{17})$	26	4800	3700	1.08
4d	$MeOBn_2NP(EO_{90}-GG_{40})$	$MeOBn_2NP(EO_{90}-GG_{40})$	30	10000	5800	1.17
5d	$MeOBn_2NP(EO_{100}-GG_{100})$	$MeOBn_2NP(EO_{100}-GG_{100})$	53	25200	5700	1.18
1dt	$H_2NP(EO_{265}-GG_{26})$	$H_2NP(EO_{265}-GG_{26})$	9	15400	8000	1.15
3dt	$H_2NP(EO_{47}-GG_{17})$	$H_2NP(EO_{47}-GG_{17})$	26	4500	3900	1.14
4dt	$H_2NP(EO_{90}-GG_{40})$	$H_2NP(EO_{90}-GG_{40})$	30	9700	5600	1.30
1t	$H_2NP(EO_{265}-IGG_{26})$	$H_2NP(EO_{265}-IGG_{26})$	9	16200	8000	1.15
3t	$H_2NP(EO_{45}-IGG_{15})$	$H_2NP(EO_{47}-IGG_{17})$	26	5000	3000	1.11
5t	$H_2NP(EO_{122}-IGG_{136})$	$H_2NP(EO_{122}-IGG_{136})$	53	27700	4400	1.13

[a] Determined from ^{1}H NMR (300 MHz, DMSO-d_6. [b] M_n determined by SEC−RI in DMF.

respective ^{1}H NMR spectra of the four different types of functional polyethers that can be synthesized after orthogonal reactions. Depending on the order of the deprotection reactions that can be chosen freely due to their orthogonal character, it is on the one hand possible to obtain P(EO-*co*-GG)-copolymers with glyceryl side chains, where the terminal amine still carries the benzyl protective groups, but on the other hand also P(EO-*co*-IGG)-copolymers with a cleaved amine in terminal position and isopropylidene-protected glyceryl units along the backbone are accessible. Both polymer types can finally be converted into the fully (terminal and in-chain) deprotected polymers (Figure 2).

The different possible copolymer structures have also been investigated by MALDI−ToF mass spectrometry. The recorded spectra obtained are quite complex with rather low resolution, but they clearly show the expected pattern for a copolymer with a variety of different possible comonomer combinations. The change in molecular weight after acidic hydrolysis or hydrogenation can also be followed by MALDI−ToF. The corresponding spectra are given in the Supporting Information.

^{1}H NMR Copolymerization Kinetics. To investigate the copolymerization behavior of EO and IGG, we used an experimental procedure that has recently been developed in our group.[19] First a comonomer solution was transferred into a NMR tube, evacuated, cooled with liquid nitrogen, and the initiator solution was added thereafter. The cold NMR tubes were evacuated, flame-sealed, and the polymerization was carried out *in vacuo*. Because of experimental reasons the online-kinetic studies were carried out in DMSO-d_6 instead of THF, which usually serves as the solvent in the large-scale polymerizations. To examine the copolymerization

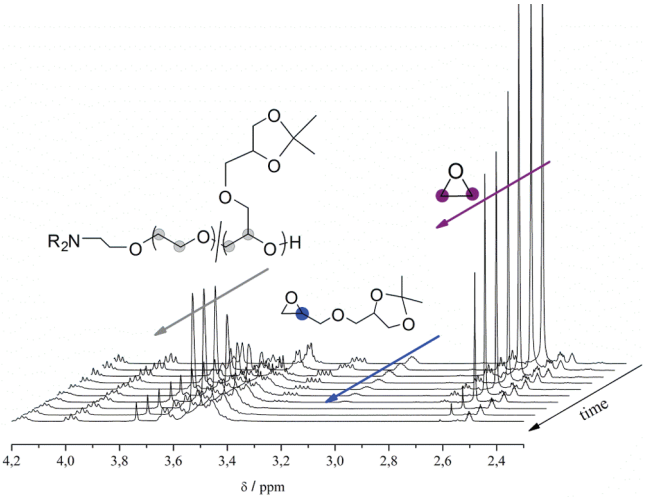

Figure 3. ^{1}H NMR spectra for the copolymerization of IGG and EO at 50 °C in DMSO-d_6 recorded after 0, 0.1, 2, 13, 21, 26, 87, 115, 190, and 264 min.

kinetics, three different temperatures, i.e., 25, 50, and 70 °C, were applied. The molecular weight distributions of all samples obtained in these online NMR experiments were narrow with PDIs around 1.06. Incorporation of the two comonomers and the growth of the polyether chain was studied by following the decrease of the epoxide signals located at 2.61 ppm for the four protons of the symmetric EO monomer and at 3.09 ppm for the methine proton of IGG, respectively. All signals are referenced to the aromatic peaks corresponding to the initiator at 6.87 ppm, which were set to 4 and should obviously remain constant in the course of the reaction. The emerging backbone signal at 3.54 ppm overlaps with different signals of the IGG monomer, which complicates the calculation of the molecular weight. This is unfortunate, since M_n determined in this independent manner could otherwise serve as an affirmation for the molecular weight calculated from the monomer decrease. Plotting the monomer conversion versus molecular weight resulted in a linear graph (see Supporting Information), confirming the living character of the polymerization, as it is expected for the anionic ROP. Figure 3 displays a zoom-in (4.5−2 ppm) of different ^{1}H NMR spectra, showing the decreasing intensity of the monomer signals and the growing backbone signal.

As expected, the rate of the polymerization is significantly influenced by the reaction temperature. While the copolymerization at 50 °C takes approximately 3.5 h to completion (5 h for the sample with higher molecular weight), approximately 1 week is required for the polymerization at 25 °C. At 70 °C, the reaction is completed already after 1 h, and even the initial spectra taken after a few seconds already reveal signals of the polymer backbone. Figure 4 shows the conversion versus time plot for EO and IGG at different temperatures, as derived from the NMR measurements.

The most relevant information clearly derived from the NMR spectra is that there appears to be little difference in the reactivity of the two monomers, despite the sterically demanding structure of IGG in comparison to EO. The conversion of both comonomers is virtually identical at all stages of the reaction (Figures 4 and 5). Unexpectedly, in the case of the two low temperature-samples (25 and 50 °C) the decrease of the IGG signal appears to be even faster at the beginning of the reaction than the decrease of the EO resonances. Figure 5 shows exemplarily the conversion of both comonomers plotted against the overall monomer-consumption for one sample at 50 °C.

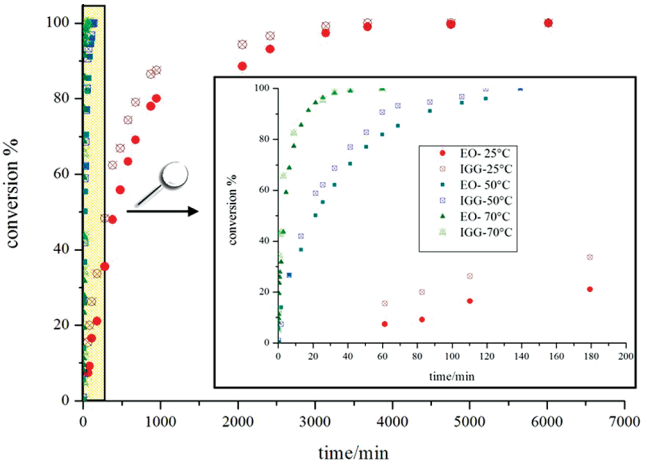

Figure 4. Monomer conversion versus time monitored by ^{1}H NMR in DMSO-*d*. resulting in polymers with the following final composition: 70 °C (green triangles) $MeOBn_2NP(EO_{61}-IGG_7)$ (**7***), 50 °C (blue squares) $MeOBn_2NP(EO_{31}-IGG_9)$, 25 °C (red, circles) $MeOBn_2NP-(EO_{29}-IGG_9)$.

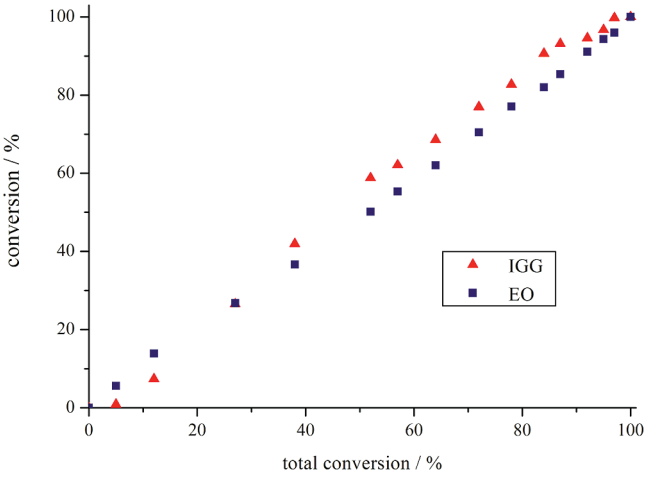

Figure 5. Momomer incorporation (percentage) versus the overall conversion at 50 °C. Final copolymer composition: $MeOBn_2P(EO_{31}-IGG_9)$.

While the decrease of EO is directly related to the total conversion, small fluctuations (to higher but also lower values) are observed for the IGG content. At this point, it should be noted that EO is the predominant component in the copolymer studied ($MeOBn_2P(EO_{31}$-$IGG_9)$) and that the EO conversion contributes to a stronger extent to the overall conversion than the conversion of IGG. Therefore, little variation of the EO-incorporation is observed. In addition, four proton signals of the two methylene groups of ethylene oxide are used to calculate the decrease of EO in the course of the polymerization, but only one methine signal is used as a reference for the determination of the IGG conversion. Obviously a larger error is expected in the latter case. Taking the above-mentioned considerations into account, it can be concluded that in all cases a linear EO and IGG conversion is observed, that is the comonomers are incorporated equally, and a random distribution is obtained in the polymer backbone. This unexpected behavior is valid independent of the EO/IGG ratio and for all temperatures studied.

^{13}C NMR Characterization. Random distribution of the comonomer units within the PEG backbone is of crucial importance with respect to potential applications of the functional PEG copolymers. ^{13}C NMR analysis permits

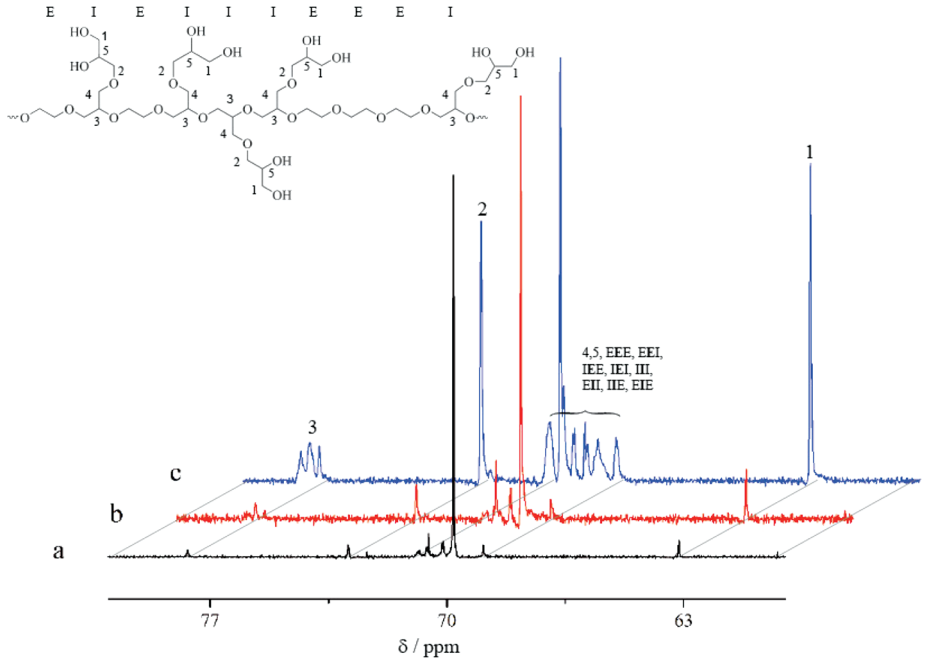

Figure 6. ^{13}C NMR spectra of different P(EO-*co*-GG) copolymers with different GG fraction of (a) 9%, (b) 14%, and (c) 53%.

Table 2. Thermal Properties of Poly(ethylene glycol-*co*-isopropylidene glyceryl glycidyl ether) and Poly(ethylene glycol-*co*-glyceryl glycerol) Random Copolymers (DSC measurements)

no.	formula	IGG/GG fraction (%)[a]	T_g[b] (°C)	T_m[c] (°C)	ΔH[d] (J/g)	T_{rc}[e] (°C)	ΔH_{rc}[f] (J/g)
1	$MeOBn_2NP(EO_{265}-IGG_{26})$	9	−54	31	35		
2	$MeOBn_2NP(EO_{180}-IGG_{32})$	14	−51	31	13		
3	$MeOBn_2NP(EO_{47}-IGG_{17})$	26	−55				
4	$MeOBn_2NP(EO_{90}-IGG_{40})$	30	−50				
5	$MeOBn_2NP(EO_{122}-IGG_{136})$	53	−49				
6*	$MeOBn_2NP(EO_{85}-IGG_8)$	9	−58	13	39	−33	34
7*	$MeOBn_2NP(EO_{61}-IGG_7)$	10	−59	14	49	−38	33
8*	$MeOBn_2NP(EO_{31}-IGG_9)$	23	−51				
1d	$MeOBn_2NP(EO_{265}-GG_{26})$	9	−48	44	45	−27	28
2d	$MeOBn_2NP(EO_{180}-GG_{32})$	14	−42	35	18	−14	17
3d	$MeOBn_2NP(EO_{47}-GG_{17})$	26	−38				
4d	$MeOBn_2NP(EO_{90}-GG_{40})$	30	−32				
5d	$MeOBn_2NP(EO_{100}-GG_{100})$	53	−28				

[a] Determined from ^{1}H NMR (300 MHz, DMSO-d_6). [b] Glass transition temperature, in °C. [c] Melting temperature T_m, in °C. [d] Melting enthalpy, in J/g, determined by integration. [e] Recrystallization temperature T_{rc}, in °C. [f] Recrystallization enthalpy, in J/g.

to investigate the monomer triad sequence distribution, revealing details concerning the incorporation statistics of IGG units. Besides the well-established signal assignment for random copolymers based on propylene oxide and ethylene oxide,[22] only few other oxirane monomer combinations have been investigated to date. However, EO has often been assumed to possess considerably higher reactivity than other epoxide monomers, such as glycidyl ethers. To confirm random incorporation, the deprotected copolymer samples were investigated, since fewer side group resonances overlap with the triad signals in question than in the respective acetal-protected copolymers. Figure 6 shows a section of the ^{13}C NMR spectra of samples **1**, **2**, and **5** with increasing comonomer fraction from spectrum a (front) to c. To keep abbreviations short for the triad sequences, the EO unit is referred to as **E** and the GG (former IGG)-units are indicated as **I**.

Two of the side group signals (1 and 2 in Figure 6) resulting from the glycerol unit are located at 63.2 and 72.9 ppm, the other two (4 and 5) overlap with the triad sequence signals of either the two methylene carbon atoms of EO or the one of the GG unit. Several microstructure-related resonances in the range 71.1−68.7 ppm occur, of which one signal at 69.9 ppm can clearly be assigned to the **E**E**E** triad. This signal decreases with increasing GG content, while other triad signals become more pronounced. In addition the signal at 68.9 ppm, which can clearly be assigned to the methylene carbon in proximity of a GG unit (for example I**E**E) does not only increase, but is split up into several signals with increasing amount of GG units incorporated (increasing abundance of I**E**I, I**I**E, and I**I**I triads). The same observations are made for the methine carbon of the GG units. The sample with the lowest GG-content shows only one single peak that is assigned to the E**I**E triad. This resonance also splits up with increasing GG-content, and the sample with 53% comonomer content shows three signals of different intensities, which is most probably explained by the occurrence of the I**I**I, E**I**I, and I**I**E as well as the E**I**E triads. The two possible end group signals of the primary or secondary carbons linked to the terminal hydroxyl groups cannot be discerned in the spectra due to the low concentration and high molecular weight of the samples. Although unequivocal assignment of all triad signals was not possible, the spectra permit to exclude the formation of longer runs of one comonomer. All observations confirm random incorporation of the IGG/GG comonomer units in the PEG backbone and are in line with the observations from the kinetic studies (vide supra).

Table 3. Comparison of the Characterization Data of the Initial Polymer, the Deprotected Material and the Benzyl Derivatives

no.	formula	M_n(NMR)[a]	M_n(SEC)	PDI	T_g (°C)[b]	T_m (°C)[c]	ΔH (J/g)[d]
1	$MeOBn_2NP(EO_{265}-IGG_{26})$	16500	7600	1.11	−54	31	35
1d	$MeOBn_2NP(EO_{265}-GG_{26})$	15700	9200	1.15	−48	44	45
1b	$MeOBn_2NP(EO_{265}-PDG_{26})$	18100	7400	1.16	−49	26	36
3	$MeOBn_2NP(EO_{47}-IGG_{17})$	5300	3000	1.08	−55		
3d	$MeOBn_2NP(EO_{47}-GG_{17})$	4800	4000	1.08	−38		
3b	$MeOBn_2NP(EO_{47}-PDG_{17})$	6400	3000	1.08	−31		

[a] Determined from ^{1}H NMR (300 MHz, DMSO-d_6). [b] Glass transition temperature. [c] Melting temperature T_m. [d] Melting enthalpy in J/g determined by integration of the melting peak.

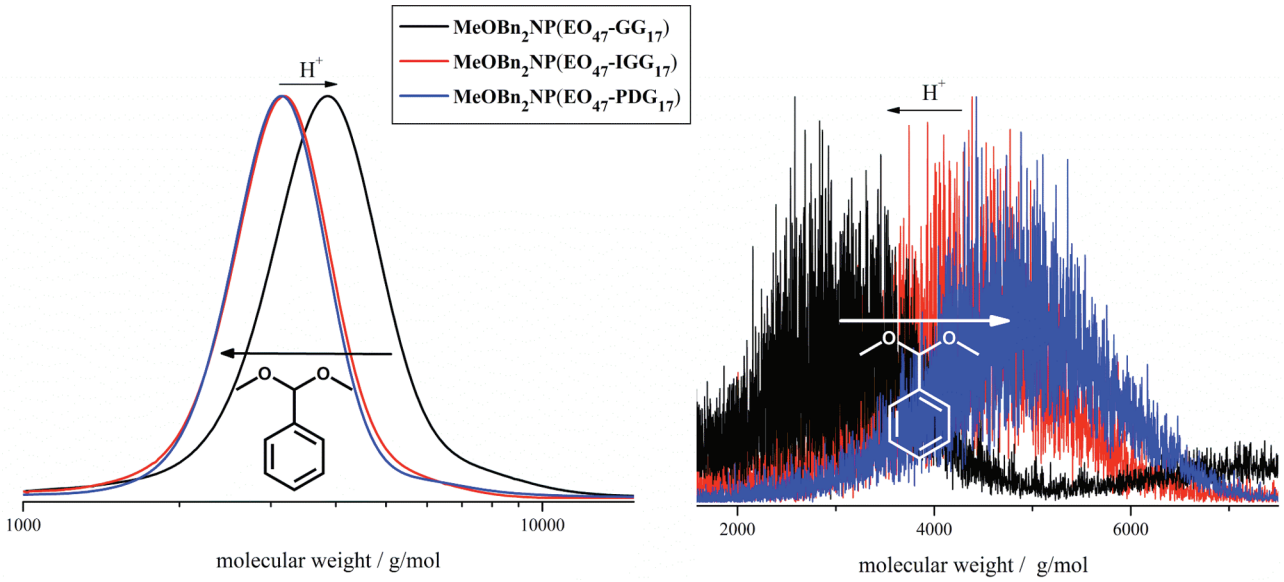

Figure 7. Molecular weight distribution of the samples **3**, **3d**, and **3b** from (a) SEC-measurements in DMF and (b) MALDI−ToF mass spectrometry using trifluoroacetate as a cationizing agent and dithranol (1,8,9-trishydroxyanthracene) as a matrix.

Thermal Behavior. The thermal properties of the P(EG-*co*-GG) copolymers are of central interest for future applications in the biomedical field as well as for use as polymer supports for organic synthesis. The thermal characteristics summarized in Table 2 have been studied using differential scanning calorimetry (DSC). The glass transition temperature (T_g) of all samples is higher than for the PEG-homopolymer (−64 °C[23] for MPEG-1000). The T_g is −54 °C for sample **1** with an IGG content of 9% and increases slightly with increasing IGG incorporation (sample **5** with 53% IGG exhibits a T_g of −49 °C). For the samples with lower molecular weights obtained from the ^{1}H NMR kinetic experiments, the T_gs were somewhat lower compared to those of higher molecular weight, but similar IGG content, which is consistent with expectation. The deprotected analogues exhibit glass transitions that are approximately 5−10 °C higher than those of the respective protected polymers, which we ascribe to hydrogen bonding interaction of the 1,2-diol side chains.

Poly(ethylene oxide) is a crystalline polymer with a melting temperature of 66 °C.[24] With increasing comonomer content (IGG or GG), T_m is gradually shifted to lower temperatures, until crystallization is completely inhibited, if the incorporated comonomer fraction exceeds 15−20%. For the P(EO-*co*-IGG) copolymer series crystallization can be observed up to an IGG content of as much as 14%, however, the melting temperature is significantly lowered in comparison to PEG (31 vs 66 °C for the homopolymer). The same observations are made for the deprotected samples, but in this case the melting temperatures are higher and additionally the melting enthalpies exceed those of the protected samples. Thus, a higher fraction of crystalline domains is present, which we ascribe to the lower steric hindrance of the glyceryl units in comparison to the bulky 1,2-isopropylidene glyceryl units, which appear to strongly impede ordering of the chains.

Derivatization. The use of MPEG (5000 g/mol) as soluble polymeric support in organic synthesis is a widely established method and is also conducted on an industrial scale.[25−28] Its success as a soluble support is based on its good solubility in water and various other organic solvents, but on the other hand good precipitability in diethyl ether and 2-propanol.[29] However, PEG exhibits low loading capacity, since it possesses only two end groups. It has been suggested that this drawback can be overcome by using hyperbranched poly(glycerol) (*hb*PG),[30] which carries multiple hydroxyl groups in either linear or terminal positions. Different reactions have been carried out using PG as support for reagents or catalysts and utilizing either the single hydroxyl-functionalities[31] or the vicinal position[32] of the terminal OH groups. To demonstrate the potential of the synthesized copolymers as soluble polymeric support by the reaction with ketones or aldehydes to the respective acetals, we employed the dimethoxyacetal derivative of benzaldehyde as a model compound. Removing the evolving methanol in the course of the reaction favors the formation of the polymeric acetal without cross-linking and leads to high yields, which is evidenced by the absence of hydroxyl signals in the ^{1}H NMR. After dialysis of the crude product, quantitatively acetalized polymers were obtained. Table 3 summarizes the characterization data of the initial and the new polymers with 2-phenyl-1,3-dioxolane (PDG) side groups.

The products were characterized by ^{1}H NMR spectroscopy. The newly emerging acetalic proton leads to signals at 5.78 and 5.69 ppm, and by integration of those and the aromatic signals of the initiator as well as the new aromatic side chains, quantitative derivatization can be confirmed. Corresponding NMR spectra are shown in the Supporting Information. The molecular weights obtained from SEC measurements, which should increase by about 88 g/mol per GG unit decreases slightly, which is consistent with the previously discussed observations made for the IGG copolymers. Figure 7 shows the shift of the molecular weight obtained from SEC-experiments and the corresponding spectra obtained by MALDI−ToF, confirming the dependence of the apparent molecular weight on the presence of the hydroxyl groups. The MALDI−ToF spectra was depicted, although the complexity of the situation does not allow for distinct assignment of all peaks, but qualitative information regarding the molecular weight can be gained. The glass transition temperature increases significantly by exchanging the isopropylidene side group with a benzylidene side group. Melting enthalpy and melting points are slightly lower in the case of the PDG-species.

Conclusion. A novel class of poly(ethylene glycol)-based random copolymers with predetermined amount of glycerol side chain functionalities, low polydispersities as well as adjustable molecular weights have been synthesized and characterized in detail, focusing on macroscopic materials properties and microstructure. The copolymerization kinetics was investigated by ^{1}H NMR spectroscopy using a recently developed online NMR technique, and ^{13}C NMR measurements were employed to support random incorporation of the two comonomers. Differential scanning calorimetry was carried out for all samples confirming expectation for the thermal properties of random copolymers. Incorporation of the recently developed monomer 1,2-isopropylidene glyceryl glycidyl ether (IGG) allows to obtain one glycerol per comonomer unit upon acidic hydrolysis. Each glyceryl unit offers two vicinal hydroxyl groups, which can serve as diol-component in the reversible formation of a cyclic acetal/ketal. In contrast to *hb*PG, which is used as polymeric support, the number of vicinal hydroxyl groups is adjustable rather independent of the molecular weight of the whole polymer.

This reaction can be used, as it has been shown exemplarily with benzaldehyde, to attach and release molecules that bear aldehyde or ketone functionality. The use of the new initiator *N,N*-di(*p*-methoxybenzyl)aminoethanol leads to the facile introduction of a terminal amino group, which can be recovered by catalytic hydrogenation subsequent to the polymerization. In addition the reaction conditions applied allow to liberate the terminal amino moiety without removal of the acetal protecting groups. This means the in-chain functional groups and the terminal group are orthogonally protected and can be addressed selectively, which is interesting with respect to a variety of applications for bioconjugation, surface modification, and drug transport and release.

Acknowledgment. The authors thank Dr. Mihail Mondeshki for NMR measurements and Alina Mohr for technical assistance. C.M., F.W., and B.O acknowledge the POLYMAT graduate school of excellence in the context of MAINZ for valuable financial support. B.O. also acknowledges the Fonds der Chemischen Industrie for a scholarship. F.W. thanks the Alexander-von-Humboldt Foundation for a fellowship. H.F. acknowledges the SFB 625 of the DFG for valuable support.

Supporting Information Available: Additional characterization data (Figures S1−S6). This material is available free of charge via the Internet at http://pubs.acs.org.

References and Notes

(1) Harris, J. M. *Poly(ethylene glycolChemistry: Biotechnical and Biomedical Applications*; Plenum Press: New York, 1992.
(2) Harris, J. M.; Zalipsky, S., *Poly(ethylene glycol- Chemistry and Biological Applications*; American Chemical Society: Washington, DC, 1997.
(3) Fruijtier-Pölloth, C. *Toxicology* **2005**, *214*, 1–38.
(4) Abuchowski, A.; Vanes, T.; Palczuk, N. C.; Davis, F. F. *J. Biol. Chem.* **1977**, *252*, 3578–3581.
(5) Davis, F. F. *Adv. Drug Delivery Rev.* **2002**, *54*, 457–458.
(6) Thompson, S.; Vadala, T. P.; Vadala, M. L.; Lin, Y.; Riffle, J. S. *Polymer* **2008**, *49*, 345–373.
(7) Wurm, F.; Räder, H. J.; Frey, H. *J. Am. Chem. Soc.* **2009**, *131*, 7954–7955.
(8) Fitton, A.; Hill, J.; Jane, D.; Miller, R. *Synthesis* **1987**, 1140–1142.
(9) Taton, D.; Le Borgne, A.; Sepulchre, M.; Spassky, N. *Macromol. Chem. Phys.* **1994**, *195*, 139–148.
(10) Halacheva, S.; Rangelov, S.; Tsvetanov, C. *Macromolecules* **2006**, *39*, 6845–6852.
(11) Dworak, A.; Panchev, I.; Trzebicka, B.; Walach, W. *Macromol. Symp.* **2000**, *153*, 233–242.
(12) Dworak, A.; Baran, G.; Trzebicka, B.; Walach, W. *React. Funct. Polym.* **1999**, *42*, 31–36.
(13) Dimitrov, P.; Hasan, E.; Rangelov, S.; Trzebicka, B.; Dworak, A.; Tsvetanov, C. B. *Polymer* **2002**, *43*, 7171–7178.
(14) Pang, X.; Jing, R.; Huang, J. *Polymer* **2008**, *49*, 893–900.
(15) Yu, Z.; Li, P.; Huang, J. J. *Polym. Sci., Part A: Polym. Chem.* **2006**, *44*, 4361–4371.
(16) Mangold, C.; Wurm, F.; Obermeier, B.; Frey, H. *Macromol. Rapid Commun.* **2010**, *31*, 258–264.
(17) Erberich, M.; Keul, H.; Möller, M. *Macromolecules* **2007**, *40*, 3070–3079.
(18) Li, Z.; Chau, Y. *Bioconjugate Chem.* **2009**, *20*, 780–789.
(19) Obermeier, B.; Wurm, F.; Frey, H. *Macromolecules* **2010**, *43*, 2244–2251.
(20) Wurm, F.; Nieberle, J.; Frey, H. *Macromolecules* **2008**, *41*, 1909–1911.
(21) Hofmann, A. M.; Wurm, F.; Hühn, E.; Nawroth, T.; Langguth, P.; Frey, H. *Biomacromolecules* **2010**, *11*, 568–574.
(22) Hamaide, T.; Goux, A.; Llauro, M. F.; Spitz, R.; Guyot, A. *Angew. Makromol. Chem.* **1996**, *237*, 55–57.
(23) Lestel, L.; Guegan, P.; Boileau, S.; Cheradame, H.; Laupretre, F. *Macromolecules* **1992**, *25*, 6024–6028.
(24) Mandelkern, L. *Chem. Rev.* **1956**, *56*, 903–958.
(25) Dickerson, T. J.; Reed, N. N.; Janda, K. D. *Chem. Rev.* **2002**, *102*, 3325–3344.
(26) van Heerbeek, R.; Kamer, P. C. J.; van Leeuwen, P. W. N. M.; Reek, J. N. H. *Chem. Rev.* **2002**, *102*, 3717–3756.
(27) McNamara, C. A.; Dixon, M. J.; Bradley, M. *Chem. Rev.* **2002**, *102*, 3275–3300.
(28) Bergbreiter, D. E. *Chem. Rev.* **2002**, *102*, 3345–3384.
(29) Lu, J.; Toy, P. H. *Chem. Rev.* **2009**, *109*, 815–838.
(30) Sunder, A.; Hanselmann, R.; Frey, H.; Mülhaupt, R. *Macromolecules* **1999**, *32*, 4240–4246.
(31) Roller, S.; Siegers, C.; Haag, R. *Tetrahedron* **2004**, *60*, 8711–8720.
(32) Hebel, A.; Haag, R. *J. Org. Chem.* **2002**, *67*, 9452–9455.